

# Small and large-scale experimental studies of soil-arch interaction in masonry bridges

M. Gilbert and C.C. Smith

*University of Sheffield, Department of Civil & Structural Engineering, Sheffield, UK*

J. Wang

*University of Salford, School of Computing, Science and Engineering, UK*

Ph. A. Callaway

*Network Rail, York, UK*

C. Melbourne

*University of Salford, School of Computing, Science and Engineering, UK*

**ABSTRACT:** The interaction between the arch, its backfill and any applied surface load is complex, and only a limited amount of relevant experimental research has been undertaken to date. Small-scale tests, which are inexpensive and quick to perform, have recently been used to try to separate the effects of load-spreading and passive restraint, whilst full-scale model bridges (3m span and housed in a large, 8.3 m long  $\times$  2.1 m high and extremely stiff test chamber), have been used to furnish high quality test data which can be correlated against numerical models, being developed in parallel. Both small and full-scale bridges are being tested in chambers incorporating large observation windows along one face to permit digital imaging and quantitative measurements of the soil and arch movements, allowing subsequent correlation with numerical models. Key results are presented, including those from full-scale model bridges filled with crushed limestone and/or soft clay.

## 1 INTRODUCTION

Whilst soil-arch interaction is now known to have a significant influence on the load carrying capacity of a typical soil-filled masonry bridge, in existing masonry arch bridge analysis / assessment procedures the backfill material is typically modelled indirectly, with simplified models being used to control the amount of live load spreading and the magnitude and form of the passive restraining pressure distribution (resisting sway of the arch into the fill). A significant simplifying assumption is that the fill pressures computed using such models are generally assumed not to depend on the mode of response of the bridge. Furthermore, whilst many models have been calibrated against test data from laboratory bridges, almost all laboratory bridges tested to date have been constructed between rigid abutments and have been backfilled with granular soil (e.g. Melbourne and Gilbert 1995, Sumon 2005). In contrast, recent intrusive investigations performed on local authority owned bridges in the UK have frequently identified that abutments are relatively insubstantial (e.g. of comparable thickness to the arch barrel), and that clay backfill is present. The need for experimental data covering a wider range of bridge types is therefore clear. To address this, a programme of small and full-scale plane strain model laboratory tests has been initiated.

Although capable of providing high quality data, full-scale laboratory arch bridge tests can be time-consuming and expensive to perform. In contrast small-scale bridges are inexpensive and quick to build and test (as noted by e.g. Fairfield and Ponniah 1994). However scaling laws mean that stresses in a small-scale bridge will be unrepresentative of those in a full-scale bridge, making small-scale modelling of certain behaviour problematic. In an attempt to remedy this, centrifuge modelling has found favour recently (e.g. Burroughs et al. 2002). In centrifuge tests small-scale bridges are accelerated to several  $g$  to ensure stresses are representative. However, modelling of clay and compacted backfill remains challenging and there are additional problems associated with scaling masonry parameters. Hence here it was decided that for convenience 1g

small-scale models would be used, but that, to minimise the influence of stress-level related issues, the arch barrel would be composed of rigid blocks separated by frictional interfaces, and that only frictional soil would be used at this scale. Several studies have been performed using this apparatus (e.g. Hulet et al. 2006) and in this paper a study concerned with direct separation of passive and load spreading effects is briefly described.

To obtain really high quality data there is no substitute for full-scale tests, and new test infrastructure has been developed to enable 3m span bridges to be tested in the laboratory; the first two pilot tests performed are briefly described in this paper. Since the plane strain soil-arch interaction problem is still poorly understood this, rather than the more complex 3D problem, was investigated, with special efforts made to ensure effectively rigid and frictionless side boundary walls. Additionally it was decided that the in-plane arch abutment fixity conditions should be fully controllable. Furthermore, in previous laboratory tests (e.g. Melbourne and Gilbert 1995) it was often found that interpreting the output from soil pressure cells could be problematic. For example, very different pressure histories were frequently obtained from two pressure cells in close proximity to each other, but the reason for this was often unclear. Interpretation would be much easier if soil mass movements could also be discerned. Whilst this is not possible if conventional spandrel walls are used, this becomes possible if observation windows are instead provided at the edges of the bridge. This feature was therefore specified in the design of both the small and large-scale test rigs, also permitting use of digital imaging and particle image velocimetry (PIV) techniques to effectively automate the process of collecting soil mass movements. Such movements can then be correlated against the results from detailed numerical models, which are being developed in parallel (e.g. Gilbert et al. 2007). As well as briefly describing the test apparatus, the results collected from pilot full-scale bridge tests involving clay and crushed limestone fill are compared and contrasted.

The main features of the small-scale and full-scale bridges which will be referred to in the paper are summarised in Table 1.

Table 1 : Comparison of small and large-scale test bridges

Parameter		Small-scale bridges	Full-scale bridges
Geometry	Span (mm)	380	3000
	Rise (mm)	85	750
	Barrel thickness (mm)	28	215
	Crown fill depth (mm)	36	305
	Transverse width (mm)	125	Arch: 1010; Fill: 1045
	Skewback height (mm)	22	220
	Skewback length (mm)	41	320
Loading	Arrangement	Loading screw	Hydraulic jacks
	Loaded length (mm)	On fill: 38, On arch: 2	220
Backfill	Load position (mm)	94.5	Bridge 1: 750; Bridge 2: 720
	Material	Sand	Crushed limestone / clay
Masonry units	Unit weight (kN/m <sup>3</sup> )	16.5	Limestone: 19.1, Clay: 22.1
	Phi (degrees)	43.8	Limestone: 54.5, Clay: -
	Cohesion (kN/m <sup>2</sup> )	0	Limestone: 3.3, Clay: 78
	Type	Cast acrylic	Solid clay engineering (cl.A)
Mortar	Crushing strength (N/mm <sup>2</sup> )	-	154
	Unit weight (kN/m <sup>3</sup> )	13.7	23.2
	Type	None	1:2:9 (cement: lime: sand)
Mortar	Crushing strength (N/mm <sup>2</sup> )	-	1.9
	Unit weight (kN/m <sup>3</sup> )	-	14.4 – 15.4

## 2 PASSIVE RESTRAINT / LIVE LOAD SPREADING SEPARATION TESTS

### 2.1 Background

One of the perennial problems when performing a simplified analysis of an arch bridge is estimating how much of the load carrying capacity can be attributed to passive restraint effects (i.e. as the parts of the arch barrel remote from the load sway into the fill) and how much is a result

of dispersion of the live load through the fill. In an attempt to directly quantify these effects, a total of 27 simple small-scale tests have been performed with the various effects alternately switched 'on' or 'off'.

## 2.2 Description of tests and results

Figure 1 shows the test setup. To allow fill to optionally be placed only on the passive side, a keystone of extended height was used. Also, the applied load could be either applied to the surface of the fill or optionally directly onto the arch barrel. Finally the fill on the passive side could optionally be contained either side of the three-quarter point hinge so as to act as a vertical dead load only. Details of the tests are summarised on Table 2.

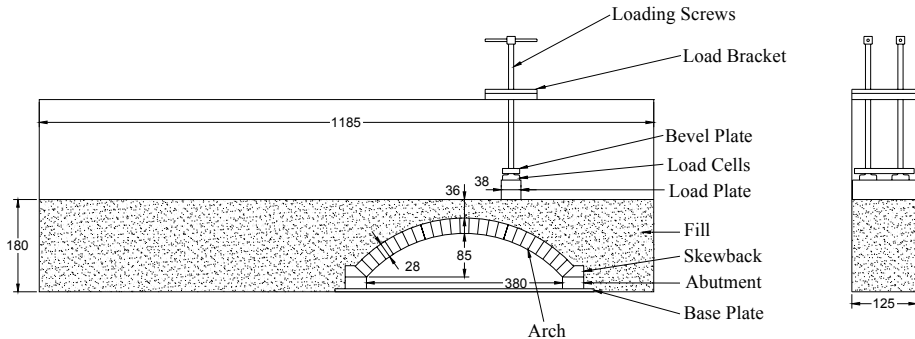


Figure 1 : Small-scale test apparatus (all dimensions in mm)

By comparing results from tests T1 [---] and T2 [-P-] and also T3 [AP-] and T5 [A--], the beneficial influence of passive restraint is clear (31% and 35% increases respectively). Similarly by comparing results from tests T3 [AP-] and T4 [APL] and also T5 [A--] and T6 [A-L] the beneficial influence of applying the live load on top of the fill is clear (32% and 29% increases respectively), although it should be noted that this increase is in part due to the increased loaded length (rather than being solely due to load spreading). Other findings were (i) that highly repeatable results could be obtained providing the testing procedure was carefully controlled, and (ii) that the extended keystone had negligible influence on the results (tests T1, T3, T4 were repeated without this and results were similar).

The experimental results were also compared with predictions obtained using the RING 1.5 analysis software (<http://ring.shef.ac.uk>). Measured geometrical and unit weight properties were used in the analyses. The simplified soil model used by RING also requires load dispersion and passive restraint properties to be set. Thus default load spreading properties were used (tests T4 [APL], T6 [A-L] only) and, following the advice in the program documentation (Gilbert 2005), the coefficient of lateral earth pressure on the passive side was increased to 1.82 (tests T2 [-P-], T3 [AP-], T4 [APL] only), corresponding to 1/3 of the classical passive earth pressure coefficient for a material with an angle of friction of 43.8 degrees. It is evident from Table 2 that the predictions are remarkably good (all within 10% of the experimental results).

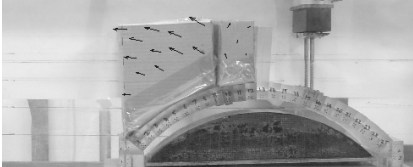
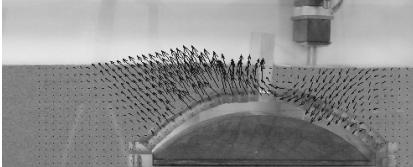
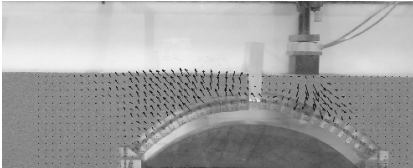
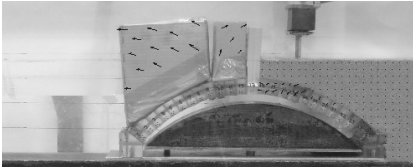
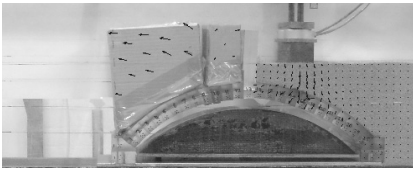
## 3 FULL-SCALE ARCH BRIDGE TESTS

### 3.1 Background

The full-scale test apparatus was designed from the outset to be capable of furnishing test data of high quality, which could then be used to verify numerical models. Some of the key differences compared with previous full-scale investigations are: (i) the enforcement of plane strain conditions through the use of effectively rigid and frictionless sidewalls; (ii) the ability to monitor individual soil particle displacements, using PIV, (iii) the use of skewbacks which could easily be fixed or allowed to slide freely; (iv) the use of clay as well as granular fill material.

Two pilot full-scale bridge tests have been performed to date, with the main initial objective being to prove the test apparatus. The first test bridge was designed to be similar to the 3m span bridges tested at Bolton in the 1990s (Melbourne and Gilbert 1995), thereby permitting direct comparison. However, unlike the Bolton bridges, which had been constructed between rigid abutments, potentially movable abutments were specified and furthermore the walls of the plane-strain test chamber marked the edges of the bridge, rather than brickwork spandrel walls as used previously. The second test bridge was designed to be identical to the first with the exception that fill material below the level of the crown of the arch was replaced with a soft clay, representative of that found in some local authority owned bridges in the UK.

Table 2 : Results from small-scale load spread / passive restraint separation tests

Test [Key*]	Photographs of model bridges with super-imposed PIV vectors at peak load	Experimental peak load capacity (N) [results without extended keystone]			RING 1.5 predicted capacity (N) [diff. cf. mean expt.]
T1 [---]		107 [104]	108 [104]	107 [106]	99 [-7%]
T2 [-P-]		141	142	140	134 [-5%]
T3 [AP-]		138 [137]	137 [135]	137 [138]	132 [-4%]
T4 [APL]		181 [178]	183 [177]	182 [179]	187 [+4%]
T5 [A--]		103	104	100	97 [-5%]
T6 [A-L]		130	131	136	136 [+3%]

\*A = Active; P = Passive; L = Load spreading

### 3.2 Details of test chamber and loading arrangement

The dimensions of the designed test chamber are shown in Fig. 2. The chamber framing was constructed using heavy duty steel I sections (406×140×39UB, Grade S275) to ensure adequate stiffness so that the plane strain conditions were maintained under load (lateral deflections were designed to be <0.1% of the soil height, i.e. less than  $\approx 2$  mm at the base). The test chamber was designed to be sufficiently long to ensure that end boundary effects would be unlikely to affect the observed failure mechanisms. Tie bars were placed across the top and bottom of the frame to provide the requisite lateral stiffness. The chamber comprises stiff walls within the steel framing, consisting of 50 mm thick plywood on the ends and on one side. On the other side, 50 mm thick acrylic windows were incorporated to allow soil displacements to be observed. Both walls had a further 6 mm layer of sacrificial acrylic sheet placed on their internal faces. To minimise side wall friction, the full faces of the 6 mm perspex sheets were covered in a layer of silicone grease followed by a 0.33 mm thick latex sheet. For normal stresses greater than 10 kPa, it has been reported (Fang et al. 2004) that this gives interface friction angles of less than  $2^\circ$ . Despite the opacity of latex, it was still possible to see the arch and fill behind. However, high contrast fill particles had to be placed at the edges of the bridge to ensure that the digital images collected had sufficient contrast.

To load the bridges two hydraulic jacks acting against a steel reaction frame were used, applying a 'line' load onto the surface of the backfill. The load was applied vertically onto the surface of the backfill through a steel loading beam (base 0.9 m×0.22 m) resting on a plywood base of the same dimensions, in turn resting on the surface of the backfill.

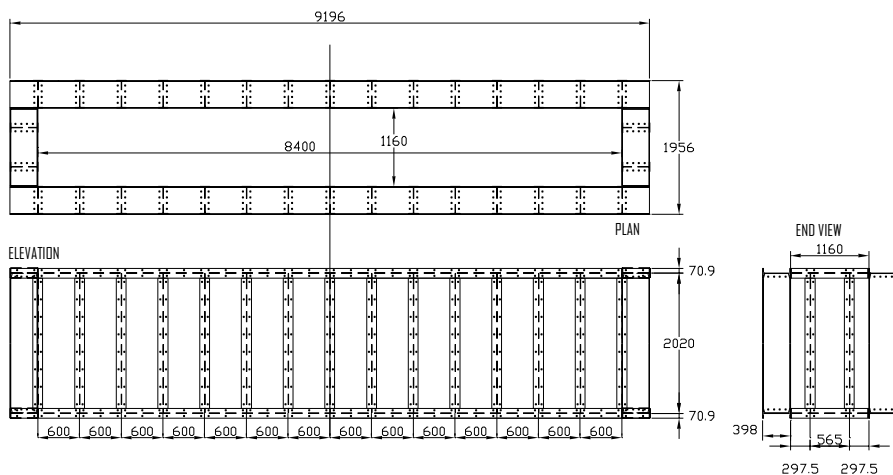


Figure 2 : Test chamber: general arrangement of steel framework (dimensions in mm)

### 3.3 Details of bridges and abutments

The arch barrels were constructed between reinforced concrete abutments. Each bridge abutment comprised two parts: a lower section bolted to the structural strong floor and an upper section (the 'skewback') mortared onto the lower section, and optionally tied to a central fixed pillar (for the first two tests the upper section was not tied but was allowed to slide freely if/when the frictional/adhesive resistance of the mortar joint between blocks was overcome).

The arch barrels were constructed on a centering with a segmental profile. The arch barrels comprised two rings constructed over a nominal width of 1010 mm, with an average clearance between the arch and the test rig sidewalls of  $\approx 15$  mm. Alternate header courses were used to prevent ring-separation from occurring during the test. The midspan points of bridge 1 and bridge 2 were located 2552 mm and 3752 mm respectively from one end of the inside of the test chamber, according to the differing anticipated soil-arch failure mechanisms.

### 3.4 Filling the bridges

The MOT Type 1 graded crushed limestone used for bridge 1 was compacted in 11No. 150 mm thick layers using a 10 kN (1 tonne) vibrating compaction plate. Coloured fill was placed against the windows to increase contrast in advance of subsequent image capture.

Bridge 2 was filled with a natural clay (firm reddish brown slightly sandy CLAY with occasional gravel with an optimum moisture content of 9%, liquid limit 29% and plastic limit 12%). The clay was wetted up in batches as appropriate to the required consistency and thoroughly mixed using the back-acting arm of a mechanical excavator. The clay was then transferred to the test rig using the excavator bucket and spread evenly using a shovel to the required layer thickness (100mm). Each layer was then compacted using a using a 10 kN (1 tonne) vibrating compaction plate. Sensitive areas adjacent to the walls and arch itself were compacted with a hand rammer. During filling, small samples were taken at regular intervals for moisture content testing. The average moisture content was 13.4% based on 95 samples (standard deviation 1.4%). To enhance the post test image analysis, limestone fines were introduced to visually contrast with the clay. Following initial placement of the clay as clods, the fines were poured into the gaps between the clods adjacent to the windows. Following compaction a clear pattern of dark and light fill was produced adjacent to the windows. Finally two 150 mm layers of limestone were placed and compacted (as described for bridge 1) over the top of the clay.

### 3.5 Test instrumentation

The middle 12 bays between the steel columns of the chamber incorporate acrylic windows and to capture soil displacements, 6No. 5 MegaPixel digital cameras were set up  $\approx 1$  m from each of these. Although in-plane displacements of the masonry and abutments can be discerned from post-processing pairs of digital images, provision of a number of Linear Variable Differential Transformer (LVDT) type displacement transducers beneath the intrados of the barrel of the test bridges enables high-precision displacement data to be obtained in real-time.

Additionally, LVDT and/or mechanical dial gauges are being used to monitor lateral movements of the test chamber, to ensure that the conditions of plane strain are met. Acoustic emission gauges were also affixed on the arch intrados. Finally, soil pressure cells were embedded in the arch extrados of the clay filled arch bridge.

### 3.6 Test results

Both bridges ultimately collapsed in the classical four-hinged failure mechanism. Fig. 3 shows the load-displacement relationships for both test bridges. It is evident that the bridge backfilled with crushed limestone had a significantly higher load carrying capacity than the bridge filled with soft clay, as might be expected.

Although at collapse hinged mechanisms formed in the case of both bridges, some abutment movement was recorded prior to this stage. In the case of the crushed limestone filled bridge spreading of the abutment remote from the applied load peaked at  $\approx 3$  mm, whilst in the case of the clay filled bridge this was significantly greater, peaking at  $\approx 8$  mm. However, in the case of the clay filled bridge rotation about the base of the lower abutment block remote from the applied load was identified, despite the fact that this had been bolted to the strongfloor. This unexpected mode of response accounted for much of the measured displacement, which was ultimately arrested by the tie connecting the top abutment block to the central pillar (to prevent this recurring, the abutment fixing detail will be modified for subsequent tests). In the case of each bridge, movement of the abutment closest to the applied loads was small,  $< 1$  mm).

Imaging and PIV processing proved very successful. Images processed using GeoPIV (White and Take 2002) for the passive side of the limestone filled bridge are shown in Fig. 4. In this case it is clear that a significant soil wedge is present, restraining sway of the arch.

Deformations of the frame were small and within the design limits set (maximum of  $\approx 0.3$  mm and  $\approx 0.8$  mm in the cases of the limestone and clay filled bridges respectively). Results of the acoustic emission studies are reported elsewhere, but indicate that acoustic emission is capable of recording crack propagation in arches with soil backfill (Melbourne and Tomor 2006).

### 3.7 Analysis of results using RING

In addition to more sophisticated analyses described elsewhere, a number of analyses were again performed using RING 1.5. The measured geometry and unit weight properties were used in the analysis (N.B. for sake of simplicity the soil unit weight for bridge 2, which was clay filled with a limestone capping layer, was taken as the mean of the limestone and clay unit weights). Additionally the simplified soil model used by RING 1.5 requires that load dispersion and passive restraint properties are set: for bridge 2 the generally conservative default values were used (a coefficient of lateral earth pressure on the passive side,  $K_p$ , of 1.0 was used, which corresponds to a weak soil whether cohesive or granular); for bridge 1 the defaults were again used except that, following the advice in the program documentation,  $K_p$  was increased to 3.25, corresponding to 1/3 of the classical passive earth pressure coefficient for a material with an angle of friction of 54.5 degrees (i.e. the measured value). In accordance with usual practice in bridge assessment the abutments were taken to be fixed. Finally the masonry crushing strength was taken as 25MPa. The analysis results are shown on Fig. 3.

It is evident that the analysis predictions are remarkably close to the experimental results. Finally, results from a further RING 1.5 analysis are also included in Fig. 3, this time using the limestone unit weight and with no live load dispersion or passive restraint. The much lower predicted strength in this case clearly illustrates the strengthening effect of the fill.

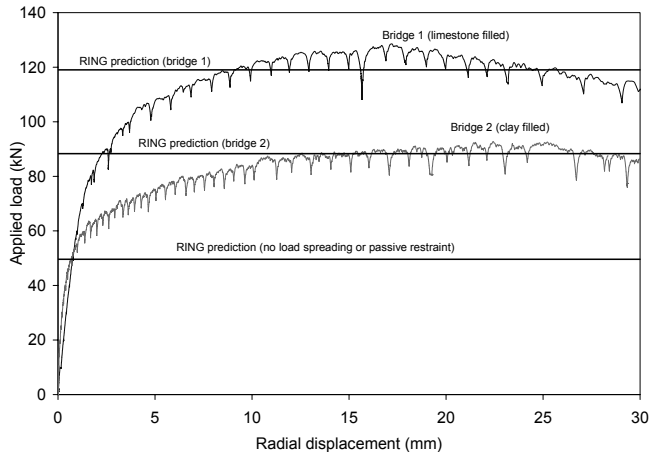


Figure 3 : Applied load vs. arch radial displacements (at quarter span)

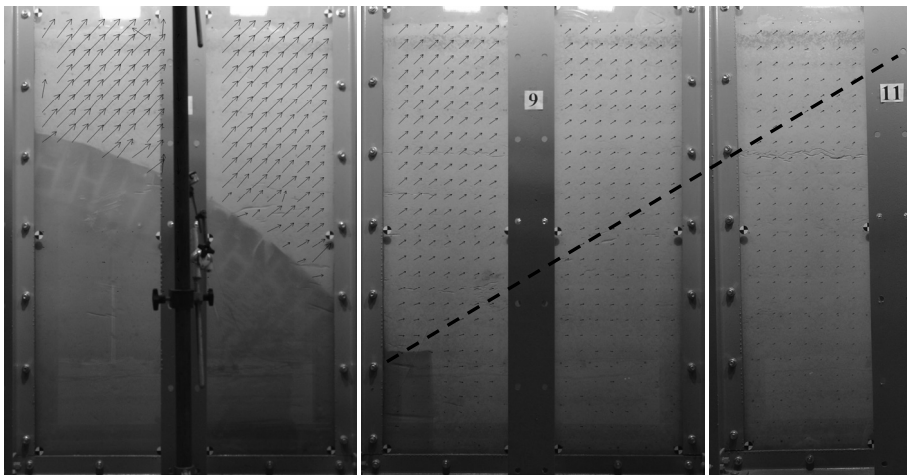


Figure 4 : Bridge 1: arch and backfill remote from the load, also showing PIV soil displacement vectors

#### 4 CONCLUSIONS

- Many masonry arch bridges in the UK contain clay backfill and abutments which are relatively insubstantial (e.g. of comparable thickness to the arch barrel). To properly investigate the behaviour of such bridges, and to further improve our understanding of granular soil-arch interaction, a new large-scale plane strain laboratory test rig has been developed, details of which are briefly outlined in the paper.
- Tests on pilot crushed limestone and clay filled bridges have been performed. The tests indicated that the test rig performed as designed, with minimal frame deflection (thereby giving effectively plane strain conditions); inclusion of large windows along one side of the test chamber permitted the acquisition of good quality particle image velocimetry (PIV) data which is being used to help better understand the nature of the soil-arch interaction.
- The limestone filled arch bridge proved capable of carrying significantly more load than its clay filled counterpart. This demonstrates the importance of the fill and indicates that performing intrusive investigation to ascertain fill type is likely to be worthwhile in the case of bridges with 'borderline' load carrying capacity.
- Both pilot bridges failed in hinged mechanisms, although some movement of the unconstrained supporting skewbacks was recorded in both cases. This was particularly pronounced in the case of the clay filled bridge.
- Small-scale tests are also being performed in parallel. These can be performed rapidly and inexpensively, and with care can provide consistent results. In this paper tests which demonstrate that both load spreading and passive restraint enhance the load carrying capacity have been briefly described.
- RING 1.5 predictions of the collapse loads of both small and large-scale test bridges were found to be remarkably good.

#### ACKNOWLEDGEMENTS

The authors acknowledge the financial support provided by Essex County Council, Network Rail and the EU Framework VI project 'Sustainable Bridges'. Thanks are also due to Mr Phil Latham for his work on setting up the full-scale test chamber, loading rig and instrumentation.

#### REFERENCES

- Burroughs, P., Hughes, T., Hee, S., and Davies, M. 2002. Passive pressure development in masonry arch bridges. *Proc. ICE, Structures & Buildings* 152(4), p. 331–339.
- Fairfield, C. and Ponniah, D. 1994. Model tests to determine the effect of fill on buried arches. *Proc. ICE Structures and Buildings* 104(4), p. 471–482.
- Fang, Y., Chen, T., Holtz, R., and Lee, W. 2004. Reduction of boundary friction in model tests. *Geotechnical Testing Journal* 27(1), p. 3–12.
- Gilbert, M., RING Theory and Modelling Guide (Version 1.5), University of Sheffield, 2005.
- Gilbert, M., Nguyen, D., and Smith, C.C. 2007. Computational limit analysis of soil-arch interaction in masonry arch bridges. *Proc. 5<sup>th</sup> International Arch Bridges Conference*, Madeira.
- Hulet, K., Smith, C.C., and Gilbert, M. 2006. The influence of flooding on the load carrying capacity of masonry arch bridges. *Proc. ICE, Bridge Engineering* 159(4), p. 97–103.
- Melbourne, C. and Gilbert, M. 1995. The behaviour of multi-ring brickwork arch bridges. *The Structural Engineer* 73(3), p. 39–47.
- Melbourne, C. and Tomor, A. 2006. Application of acoustic emission for masonry arch bridges. *International Journal of Strain Measurement* 42(3), p165–172.
- Sumon, S. K. 2005. Innovative retrofitted reinforcement techniques for masonry arch bridges. *Proc. ICE Bridge Engineering* 158(3), p. 91–99.
- White, D. and Take, W. 2002. GeoPIV particle image velocimetry (PIV) software for use in geotechnical testing. Technical Report 322, Geotechnics Group, Cambridge University Engineering Department, Cambridge.